

Martin Prachař, [martin.prachar@fsv.cvut.cz](mailto:martin.prachar@fsv.cvut.cz)

WG3 - Nuno Lopes, [nuno.lopes@ua.pt](mailto:nuno.lopes@ua.pt)

WG1 - Carlos Couto, [ccouto@ua.pt](mailto:ccouto@ua.pt)

WG3 - Michal Jandera, [michal.jandera@fsv.cvut.cz](mailto:michal.jandera@fsv.cvut.cz)

WG3 - Paulo Vila Real, [pvreal@ua.pt](mailto:pvreal@ua.pt)

WG2 - František Wald, [wald@fsv.cvut.cz](mailto:wald@fsv.cvut.cz)

## **2 LATERAL TORSIONAL-BUCKLING OF CLASS 4 STEEL PLATE GIRDERS UNDER FIRE CONDITIONS: EXPERIMENTAL AND NUMERICAL COMPARISON**

### Summary

This paper presents a validation of numerical model of the lateral torsional-buckling of Class 4 steel plate girders under fire conditions. In the framework of the RFCS project FIDESC4 - Fire Design of Steel Members with Welded or Hot-rolled Class 4 Cross-sections, three simple supported beams, one of them non-uniform (tapered), submitted to two point loads were tested with different temperatures at the Czech Technical University in Prague. Detailed information on the geometric data, measured geometrical imperfections and actual mechanical properties are given. The design of the test set-up and description of the experiment is given, as well as verification of numerical model. The experimental load-displacement diagrams and the ultimate loads were compared with the numerical results obtained with the FE software ABAQUS and SAFIR.

### **2.1 INTRODUCTION**

This paper deals with lateral-torsional buckling (LTB) of slender steel I beams under fire conditions. The fire behaviour of three beams is analysed by means of experimental tests and numerical analyses.

Steel members with thin-walled cross-sections are commonly used in buildings due to its lightness and long span capacity. However the understanding of the fire resistance of these structural elements can still be further developed and increased.

The structural steel elements with thin walled cross-sections (Class 4 section according to Eurocode 3 (CEN, 2005) subjected to uniform bending diagram, are characterized by having the possibility of occurrence of failure by both local and global buckling modes (LTB). These instability phenomena and their influence on the ultimate strength are of utmost importance to characterize the behaviour of these members. The local buckling occurs due to the compression of thin plates in profiles cross-sections (see Fig. 2.1a). The LTB is an instability phenomenon that in I-sections is induced by the



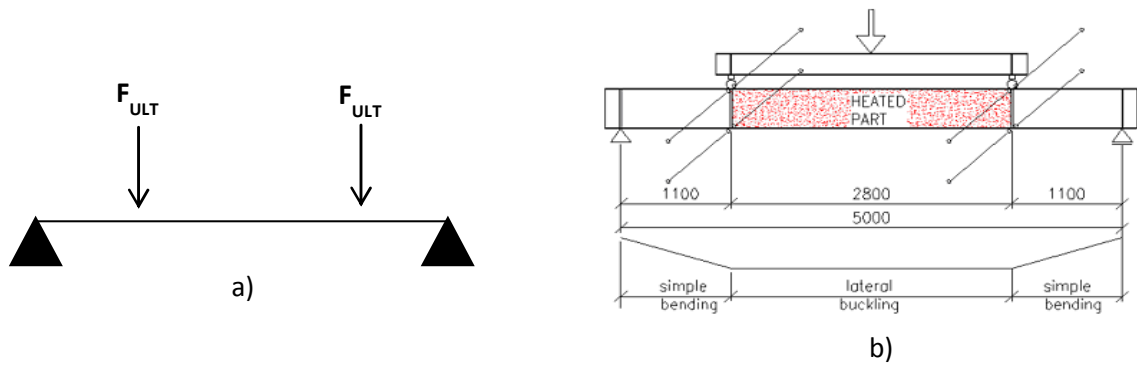
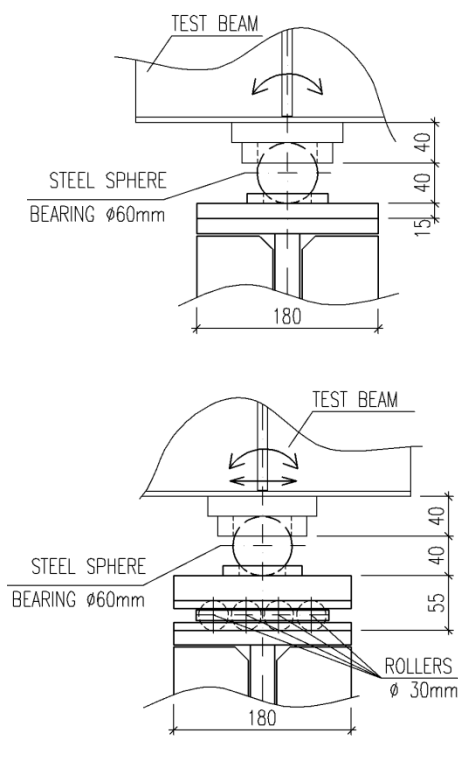


Fig.2.2 Tested beam: a) scheme; b) test set-up



a)



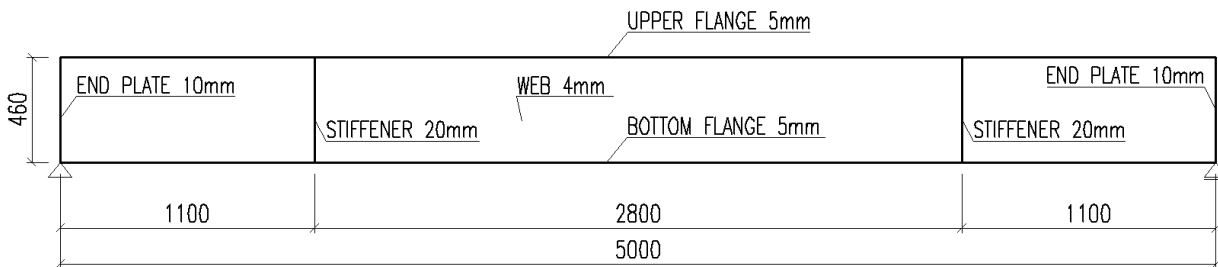
b)

Fig. 2.3 Pinned point supports: a) fixed; b) free

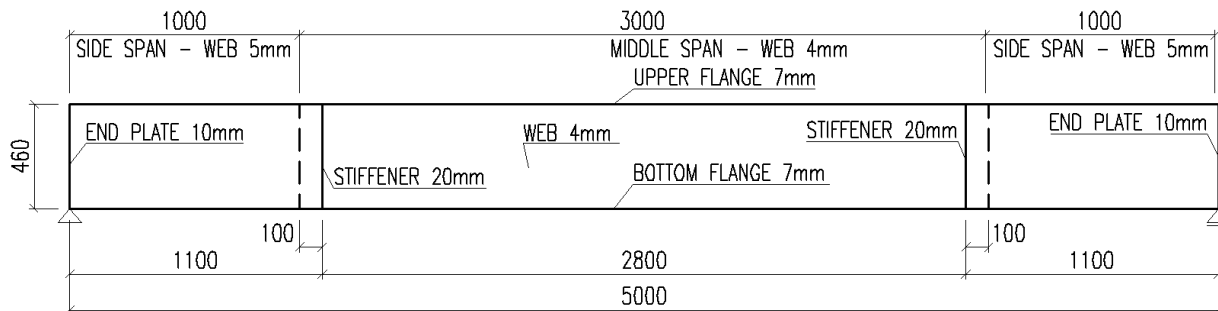
The three tests differ in the cross-sections and applied temperatures. Tab. 2.1 presents the used cross-sections which were fabricated by welding of different steel plates for the flanges and webs. The test 3 was performed on a non-uniform beam. The tests 1 and 2 were set to be at 450°C and test 3 at 650°C. End plates were used with thicknesses of 10 mm and stiffeners at the load application points had 20 mm of thickness. Figure 2.4 summarises the beams dimensions.

Tab. 2.1 Cross-sections

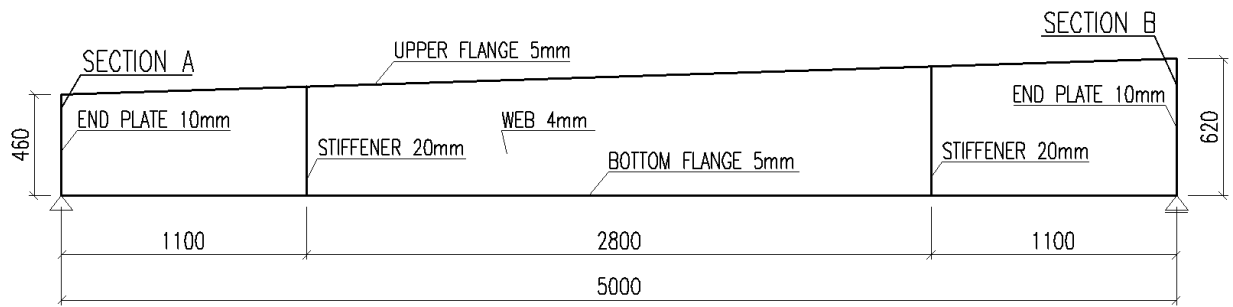
	Heated Cross-section [mm]		Non-heated Cross-section [mm]	
	Dimensions [mm]	Idealized dimensions (FEM)		
Test 1 (450°C)	$h = 460$ $b = 150$ $t_f = 5$ $t_w = 4$		The same as in the heated part See Fig. 2.4a	
Test 2 (450°C)	Middle span $h = 460$ $b = 150$ $t_f = 7$ $t_w = 4$	<u>MIDDLE SPAN</u> 	Side span $h = 460$ $b = 150$ $t_f = 7$ $t_w = 5$ (see Fig. 2.4b)	<u>SIDE SPAN</u> 
Test 3 (650°C) (Tapered beam, see Fig. 2.4c)	$h_A = 460$ $h_B = 620$ $b = 150$ $t_f = 5$ $t_w = 4$	<u>SECTION A</u> 	<u>SECTION B</u> 	



a)



b)



c)

Fig. 2.4 Beams: a) test 1 and 2; b) test 3

The real geometric imperfections, steel temperatures and mechanical properties of the steel plates were measured, as described in the following section.

### 2.3 EXPERIMENTS

In this section the tests set up and tests procedures are given in detail (see Figure 2.5). The mechanical properties, restraint conditions, geometric imperfections, temperatures in the steel and all other important parameters measurements are described. The load application on the tests was deflection controlled.

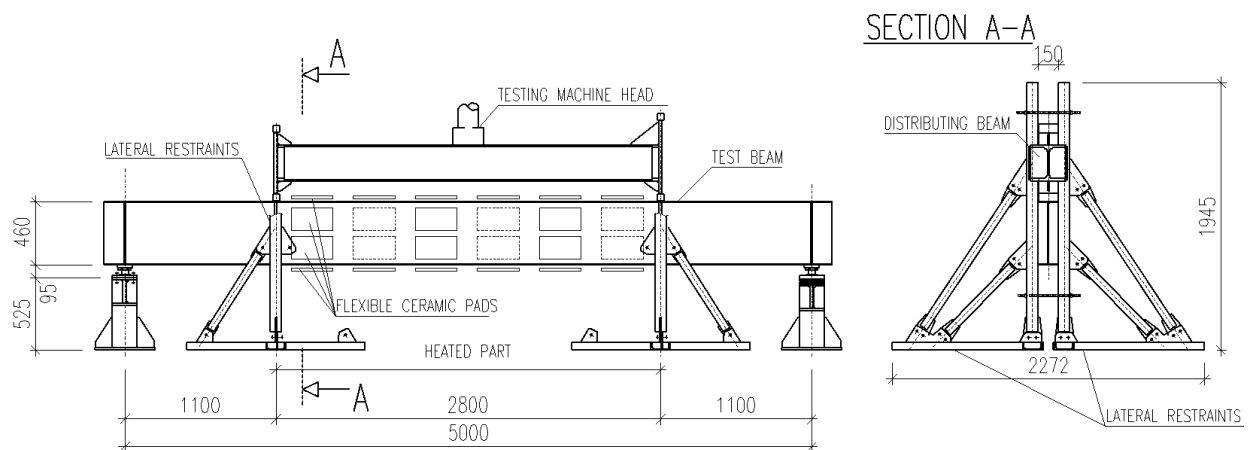


Fig. 2.5a Detailed experimental test set-up



Fig. 2.5b Detailed experimental test set-up

Within the experiment, the material properties of the plates used on the profiles were measured. Number of coupon tests was performed to determination of yield strength and young's modulus for each thickness. The real values of yield strength are presented in Table 2.2

Tab. 2.2 Steel plates yield strength

Beam parts	Yield strength [MPa]
<b>Test 1</b>	
Flanges	385
web	394
<b>Test 2</b>	
Flanges	435
web	394
Web in side span	376
<b>Test 3</b>	
Flanges	385
web	394

Before the experiment, after placing the beam on the support, (2) the initial geometry of the specimens was established by manual measurements. It consists of amplitude measurement for global and local imperfection. Amplitude of global imperfection was measured as a deviation from a string spanned between the stiffeners. For measurements of local imperfection amplitude, a special device set with a centesimal displacement meter was used. The investigation was made in compression zone of the beams only. Figure 2.6 shows the position of the measurement. Table 2.3 shows the maximum amplitude of the local and global imperfections.

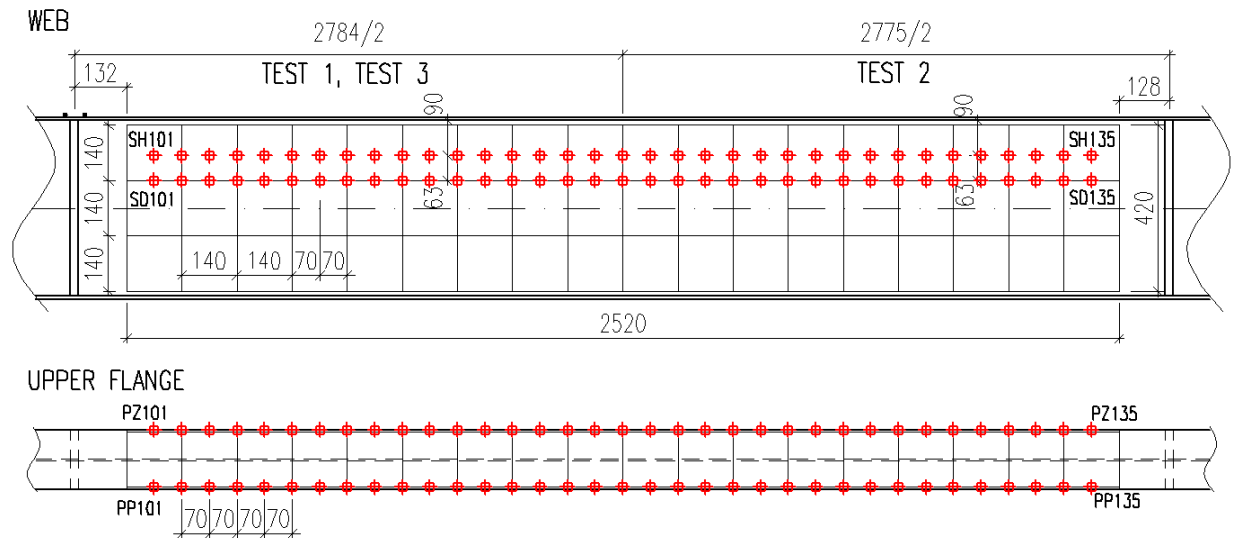


Fig. 2.6 Measured geometric imperfections - position of the measurements

Tab. 2.3 Local and global imperfections amplitudes

Imperfection	Amplitude [mm]
<b>Test 1</b>	
Local	7.36 (web)
Global (y-y axis)	2.5
<b>Test 2</b>	
Local imperfections	5.8 (web)
Global (y-y axis)	1.5
<b>Test 3</b>	
Local	7.59 (web)
Global (y-y axis)	1.5

Mannings 70kVA heat power units with 6 channels were used to heat the specimens. Cable connection of 70kVA consists of 6 triple cable sets and 4-way splitter cables can accommodate 24 flexible ceramic pads attached. Maximum connected load for the 70kVA unit is 64.8kW. One size of the ceramic pads was used: 305 x 165mm. The power output of the pad was 2.7kW. Ceramic pads were placed as shown in Figure 2.7. In the first step, the pads were put on the rod rack in order to maintain the position of the heating elements on the web. On the bottom flange, the pads were fixed with the steel wires. On the top flange, the pads were fixed by adhesive tape only.

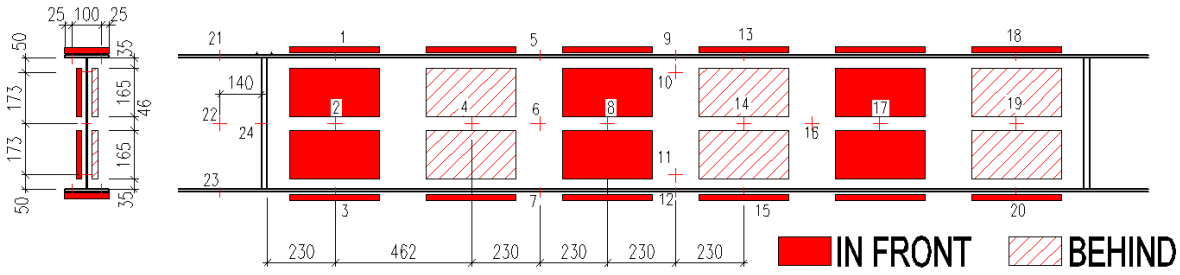


Fig. 2.7 Layout of flexible ceramic pads and thermocouples



Fig. 2.8 Test specimen

Two types of material were used for beams isolation. In the first step, the space between the flanges was filled with standard wool. The space on the flange and bellow the flange was insulated using standard wool too (ROCKWOOL Airrock HD). The wool was fixed on the beam with steel wires. In the following step, the middle span was wrapped by super wool insulation material.

Twenty-four thermocouples were used for the temperature measurement. Twenty were placed in the middle span and four were placed in the side spans for monitoring of the temperature in not-heated section. The thermocouples were distributed on the beam according to position of ceramic pads, as shown and numbered in Fig. 8. Beam temperatures were recorded from the beginning of heating to the end of experiment. The temperatures varied during the test slightly and were not uniform for the whole section. The average measured temperatures from each part of the beams can be found in Table 2.4.

Tab. 2.4 Steel temperatures

Beam parts	Average temperature (°C)
<b>Test 1</b>	
Upper flange	457
Web	444
Bottom flange	354
<b>Test 2</b>	
Upper flange	481
Web	443
Bottom flange	369
<b>Test 3</b>	
Upper flange	624
Web	567
Bottom flange	416

## 2.4 NUMERICAL ANALYSES

To consider the local buckling of thin walls in members with Class 4 cross-sections, shell finite elements were used instead of the beam finite elements, due to the fact that it is one of the dominant failure modes.

As mentioned before, two finite element programs were used, ABAQUS and SAFIR. The software SAFIR (Franssen, 2005) is a geometrical and material non-linear finite element code especially developed, at the University of Liège, to model the behaviour of structures in case of fire.

The boundary conditions applied to the model followed the degrees of freedom provided by the supports on Fig. 2.3 and the lateral restraints on Fig. 2.2b as it is presented in Fig. 2.8. On the supports, only the displacements were restrained and the rotations were set to be free.

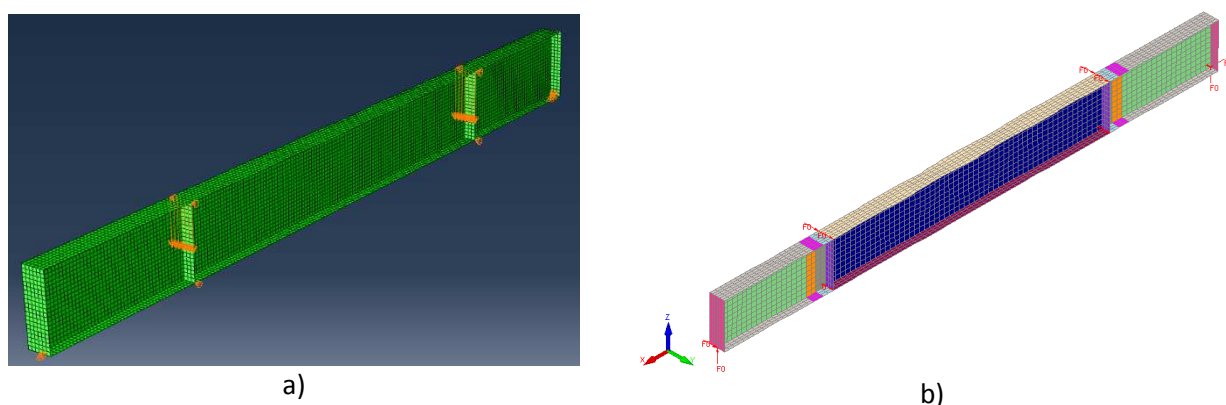


Fig. 2.9 Numerical model used: a) in ABAQUS b) in SAFIR

To obtain the models shown in Figure 2.9, a mesh convergence study was performed. The optimal number of shell elements, in the flanges and in the web, was studied. It is presented in Figure

2.10, the variation of the ultimate bearing load in function of the number of shell elements in the model. On the chosen model ten divisions on the flanges and on the web were used, the beam length was divided by 100 (Safir). Despite this mesh was found to be fine enough, width of the element (in direction of the beam length) was 25 mm for the model in ABAQUS. The welding fillets were not taken into account.

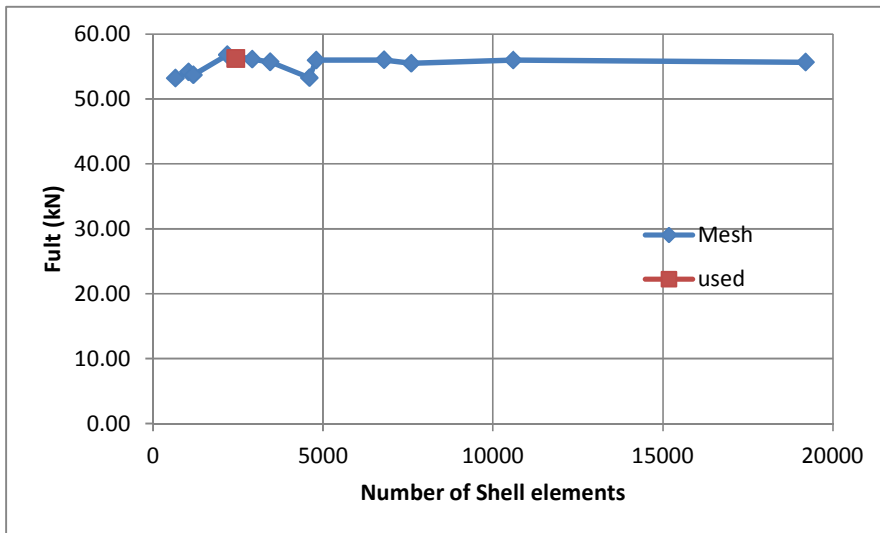
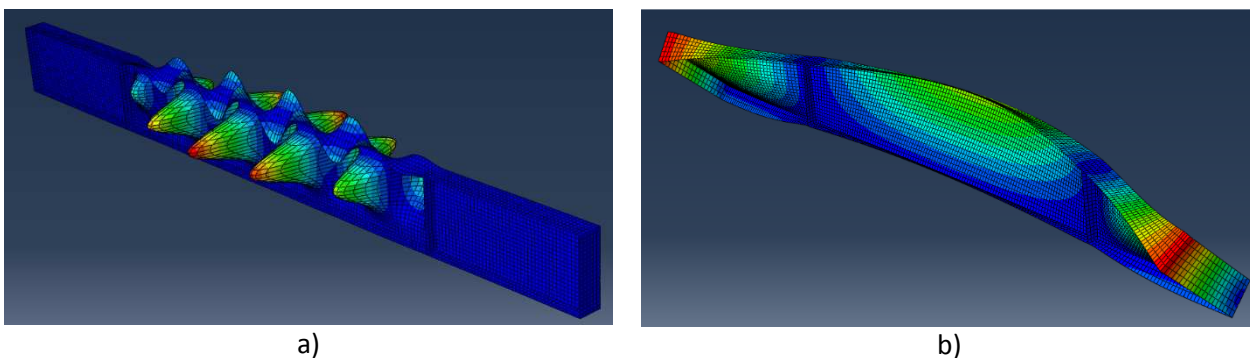


Fig. 2.10 Ultimate bearing load in function of the number of shell elements

Initial geometric imperfections were applied following the beams eigen modes. Two shapes were chosen: the beam 1st local buckling mode and 1st global buckling mode (LTB) shapes (Figure 2.11). For the imperfection amplitudes, the measured values were used (see the previous section).



a) b)  
Fig. 2.11 Beams buckling modes shape: a) local; b) global

In these numerical models it was considered that the applied loads were controlled by forces and by displacements. The consideration of the steel thermal expansion was also tested but is neglected in the study shown here. The measured values of the steel mechanical properties (yield strength and

young modulus) and the measured temperatures were adopted in the models. No residual stresses were considered.

## 2.5 DISCUSSION OF THE RESULTS

Fig. 2.12 shows the failure deformed shape of the test 1 obtained on the experimental test and on the numerical analyses.

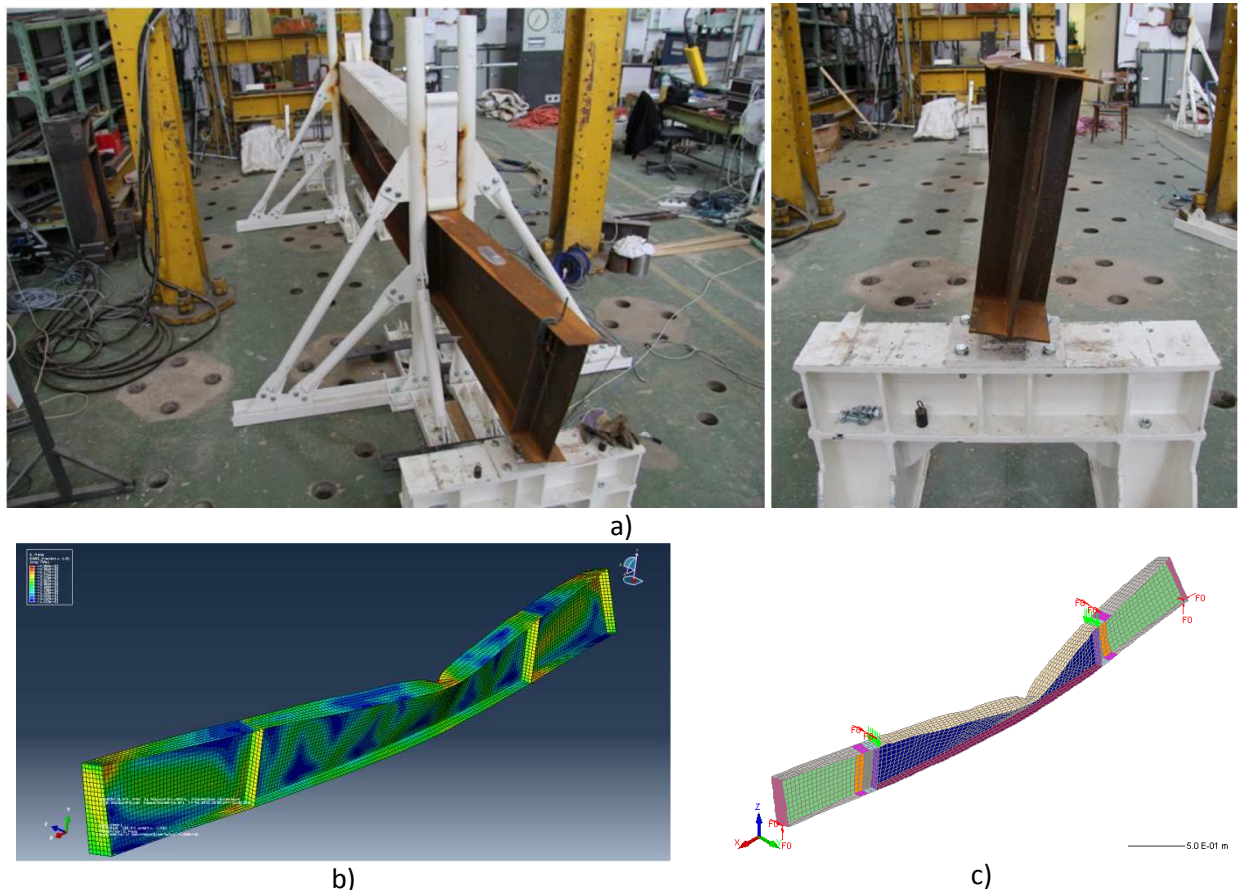


Fig. 2.12 Failure deformed shape on the: a) experimental test; b) ABAQUS analysis; c) SAFIR analysis

The numerical models approximation to the experimental tests is analysed in Figure 2.13. This figure shows the load-displacements relationship comparisons between the experimental test and the numerical analyses. The load corresponds to the total force imposed on the two load application points. The shown displacement corresponds to the vertical displacement at the bottom flange at mid span. In the graphs the curves corresponds to the results of the models with:

- DC – Controlled by displacement;
- FC – Controlled by force;
- No exp - without thermal expansion;
- exp Yes - including thermal expansion;

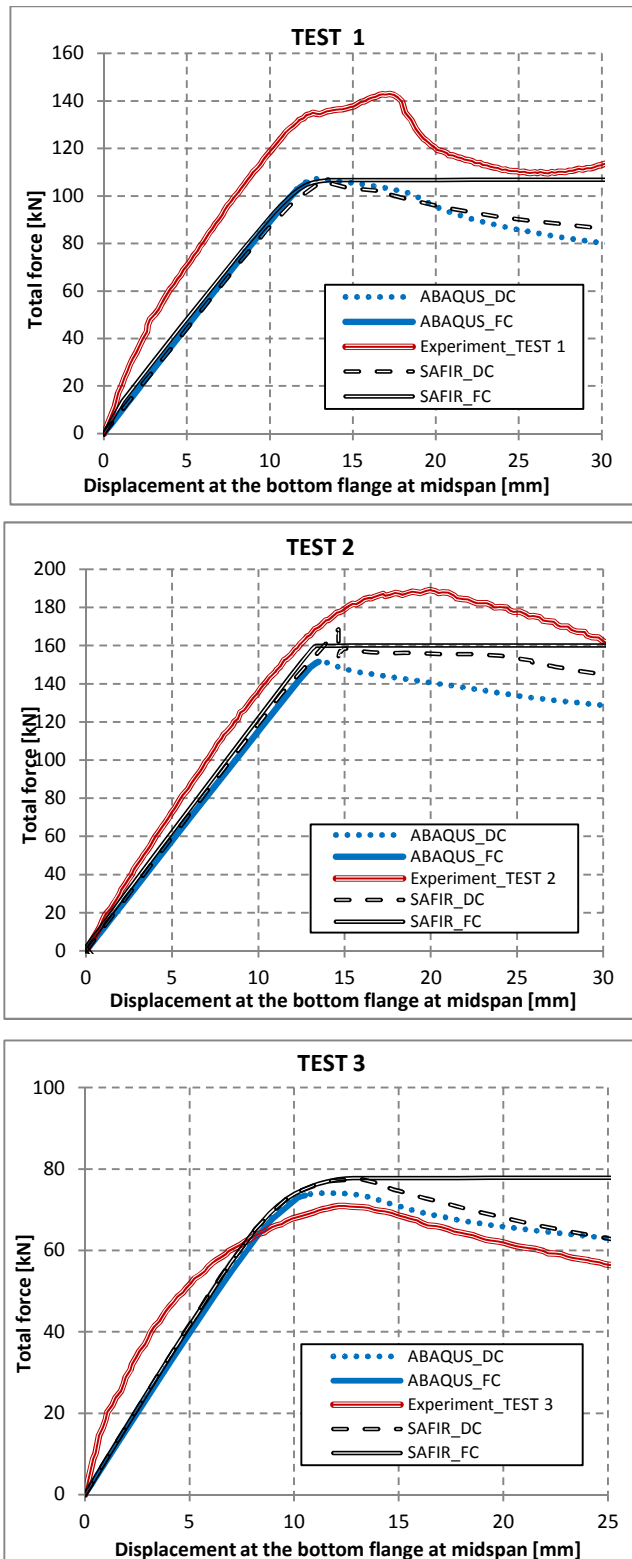


Fig. 2.13 Load-displacement relation for the three beams: experimental and numerical

From the graphs it can be concluded that the two programs give results and mechanical behaviours at high temperatures that are close from each other. The obtained experimentally initial

tangent of the curve is different from the numerical curves mainly in test 1 and 3. The maximum loads in the tests 1 and 2 are higher than the corresponded numerical tests values. Overall the approximations are reasonable considering the nature of the different parameters involved in the presented tests, as for instance the heating process.

## 2.6 SUMMARY

The paper presents numerical modelling using two different FEM software packages on three fire resistance tests to steel beams with slender I-cross-sections. The results were compared to tests and found reasonably close. Therefore, it can be concluded that the mechanical behaviour during the complete duration of the fire tests to the beams was fairly predicted by the numerical models.

### Acknowledgement

The authors would like to thank the financial support by the European Commission through the Research Fund for Coal and Steel for research project FIDESC4 "Fire Design of Steel Members with Welded or Hot-rolled Class 4 Cross-section".

### References

- ABAQUS, 2010: Abaqus, Analysis user's manual, Volumes I-IV, version 6.10. Hibbitt, Karlsson & Sorensen, Inc., Providence, R.I, USA, 2010.
- Franssen, 2005: Franssen JM, "SAFIR A Thermal/Structural Program Modelling Structures under Fire", *Engineering Journal* vol 42/3, 143-158, 2005.
- CEN, 2005: CEN European Committee for Standardisation, EN 1993-1-1, Eurocode 3, Design of Steel Structures - Part 1-1: General rules and rules for buildings, Brussels, Belgium, 2005.
- CEN, 2006: CEN European Committee for Standardisation, EN 1993-1-5, Eurocode 3: Design of Steel Structures - Part 1-5: Plated structural elements, Brussels, Belgium, 2006.
- CEN, 2011: CEN European Committee for Standardisation, EN 1090-2:2008+A1, Eurocode 3: Execution of steel structures and aluminium structures - part 2: Technical requirements for steel structures, Brussels, Belgium, 2011.
- Fidesc4 - Fire Design of Steel Members with Welded or Hot-rolled Class 4 Cross-sections, Six-monthly Report for the Research Programme of the Research Fund for Coal and Steel, September 2012.